bnhcrc.com.au

LARGE-EDDY SIMULATION OF NEUTRAL ATMOSPHERIC SURFACE LAYER FLOW OVER HETEROGENEOUS TREE CANOPIES

Peer reviewed research proceedings from the Bushfire and Natural Hazards CRC & AFAC conference
Sydney, 4 – 6 September 2017

Duncan Sutherland, Khalid A. M. Moinuddin, Andrew Ooi
Victoria University
University of Melbourne
Bushfire and Natural Hazards

Corresponding author: duncan.sutherland@vu.edu.au

Version	Release history	Date
1.0	Initial release of document	04/09/2017

Publisher:
Bushfire and Natural Hazards CRC

September 2017

Citation: Sutherland, D., Moinudding, K. A. M. & Ooi, A. (2017) Large-eddy simulation of neutral atmospheric surgace layer flow over heterogeneous tree canopies. In M. Rumsewicz (Ed.), *Research forum 2017: proceedings from the research forum at the Bushfire and Natural Hazards CRC & AFAC Conference*. Melbourne: Bushfire and Natural Hazards CRC.

Cover: New Zealand Fire Service

TABLE OF CONTENTS

ABSTRACT	3
INTRODUCTION	4
NUMERICAL METHODS	7
RESULTS AND DISCUSSION	9
CONCLUSIONS	14
ACKNOWLEDGEMENTS	15
REFERENCES	16

ABSTRACT

Large-eddy simulation of a neutral atmospheric surface layer (ASL) flow is performed over a modelled tree canopy with heterogeneous leaf-area density. The canopy is arranged as a series of equally-sized stripes of different leaf-area density, emulating the study of Bou-Zeid et al. (E. Bou-Zeid, C. Meneveau, and M.B. Parlange. Large-eddy simulation of neutral atmospheric boundary layer flow over heterogeneous surfaces: Blending height and effective surface roughness. Water Resources Research, 40(2), 2004.) over heterogeneous rough surfaces. The simulation results are analysed to understand the qualitative similarities and differences between ASL flows over heterogeneous canopies and heterogeneous roughnesses. This will allow, in the future, the identification of the equivalent roughness length, displacement length, and blending height which parameterises the flow above the heterogeneous canopy. In the present work we restrict attention to the characterisation of the four canopy case and the blending height and β parameter, the ratio of shear stress to velocity at the canopy top. The general characteristics of the four-canopy case are representative of the other cases. Strong vertical velocities (ie up- and down-drafts) exist at the interface between the heterogeneous roughness stripes. However, for a canopy, vertical velocity couplets exist on the vertical interface between two canopies. This implies the presence of sub-canopy recirculation zones at canopy interfaces, which can be confirmed by visualisation of the fluid streamlines. Above the canopy internal boundary layers form over each canopy stripe and exhibit similar features to the characteristic upstream plumes of flow over a rough surface. The shear stress immediately above the canopy varies over the stripes but it varies more smoothly over a canopy than over a heterogeneous roughness. These simulations will allow the development of parameterisations for the near-surface layer and the sub-canopy winds. A better understanding of the effect of heterogeneous canopies on the sub-canopy winds will improve predictions of the wind reduction factor, and in turn, improve operational fire spread predictions.

INTRODUCTION

Knowledge of sub-canopy winds is important for characterising wildfire spread using operational models such as the McArthur [McArthur, 1967] model. The McArthur Mk V forest model takes wind speed at 10 m from the ground in the open (ie. outside of the forest) as an input and returns the forward-rate-of-spread of a fire within a forest. The McArthur model therefore implicitly accounts for the reduction in wind speed due to the tree canopy. McArthur [1967] includes a figure showing the a correlation between the open wind speed at 33 feet (approximately 10 m) from the ground and the wind speed at 5 feet (approximately 2 m) from the ground within the forest. Three eucalyptus forests each with different stocking density and height were considered. These wind speed measurements are valid only for the conditions under which they were made, and are not valid for any given forest.

In order to compensate for different forest types, densities, heights, and so on, a wind reduction factor (WRF) is typically used when applying the McArthur model to a real-world fire in forest types different to what McArthur [1967] considered. It is unclear how to best predict the WRF a priori from the data available to fire behaviour analysts such as forest type, prevailing wind speed, and canopy height [Heemstra, 2015]. Operational forecasting tools such as Phoenix RapidFire [Tolhurst et al. 2008] also use wind reduction factors to account for the drag of different forest types. Field studies have been conducted to measure wind reduction factors for various Australian forest types [Moon et al. 2016]. Moon et al. define wind reduction factor as the ratio of open wind speed at 10 m to the sub-canopy wind speed at a range of heights. Moon et al. present numerous measurements showing the variation in WRF with sub-canopy wind measurement height and forest type, height, and age. The purpose of their study was to provide a sound scientific basis for choosing the values of WRF used in operational models.

Another approach, present in the meteorological literature for some time, is to develop reduced analytical models for wind speed profiles within an idealized canopy. For large and spatially uniform forests it appears that an analytical model, originally due to Inoue [1963], and later modified and verified by Harman and Finnigan [2007] is sufficient to predict the sub-canopy wind speed. Although, to the best of our knowledge, this model has not been trialled by fire practitioners.

Most forests are not spatially uniform and contain many inhomogeneities (or heterogeneities) in all spatial directions. The leaf area density (LAD), the amount of volume occupied by all plant matter, is often used to characterise a canopy. In realistic canopies, the leaf area density has strong vertical variation essentially because the leaves tend to be concentrated at the top of a tree canopy. Often, forest canopies will end abruptly at a man-made break in the forest or will become sparse due to some change in forest type. Additionally there are small, effectively random, variations in LAD over all directions in tree canopies due to natural variation in the vegetation. The aerial photograph (figure 1a) taken near Ararat in Victoria, Australia, shows a canopy region with some heterogeneity in between forest type 1 and forest type 2.

In reality these changes are not abrupt, regular, in one particular direction, nor always aligned with the wind. However, as a first step to characterising the wind flow over such canopies we will idealise the canopy to alternating stripes of high and low leaf area density. The flow over this heterogeneous, striped canopy will be simulated using the large eddy methodology.

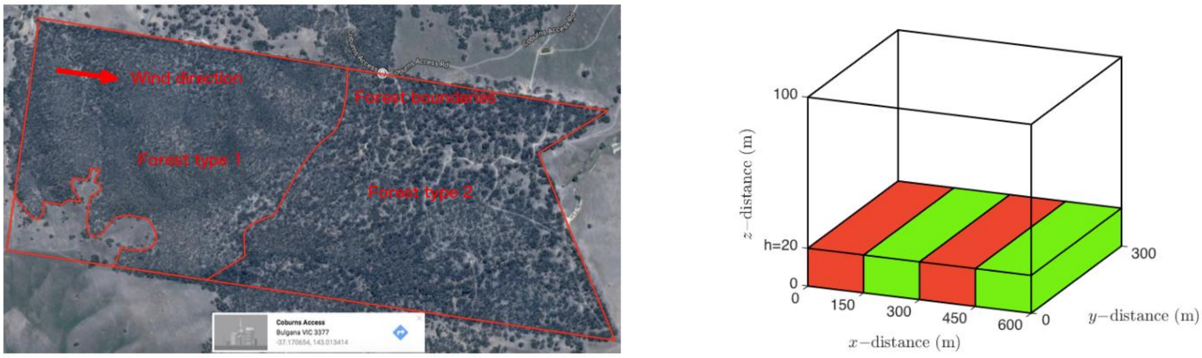

(a) (b)

Figure 1: (a) Aerial photograph taken near Ararat in Victoria showing a forest canopy with step-like variation in leaf area density between forest type 1 and forest type 2. The wind direction aligned with this step change in forest type is shown by the arrow. (b) Simulation domain for the four-canopy case. Red: $LAD = 0.2$, green: $LAD = 3$. The $x-$ and $y-$boundary conditions are periodic.

Grant et al. [2015] suggest using a canopy model has numerous advantages over simple roughness parameterisations particularly when flow separation occurs over complicated terrain. Harman and Finnigan [2007] have demonstrated that analytic canopy models and a canopy parameterisation, which in turn provide a roughness length, displacement length, and stability parameterisation can be used successfully for homogeneous forests. The aim of this work is to use Large Eddy Simulation (LES) to study the flow over heterogeneous canopies with an eye towards developing a canopy model and, subsequently, a parameterisation of the whole flow.

The code used to perform the simulations is Fire Dynamics Simulator (FDS) [McGrattan et al., 2013]. FDS has previously been benchmarked against experimental and other simulation results by Mueller et al. [2014] for flows over homogeneous canopies and canopies with finite edge boundaries. LES of flows over canopies with edge heterogeneities, where the canopy abruptly stops, have been conducted by Cassiani et al. [2008], who identified the presence of recirculation regions downstream of the canopy, and Kanani-Suhring and Raasch [2017] who studied scalar (eg. temperature, humidity, CO2) transport near the edges of the canopy. Schlegel et al. [2015] conducted simulations with heterogeneous canopies where the leaf area index profile was obtained using LiDAR of a real world forest. Comparisons to field measurements revealed that small-scale plant inhomogeneities considerably influenced the observed flow statistics. In the present work we conduct idealised numerical experiments to identify how the effective roughness length, displacement length, and blending height vary above the heterogeneous canopy.

Similarly we aim to examine the features of the sub-canopy flow. A greater understanding of the effect of heterogeneous canopies will improve fire spread prediction, extend previous wind reduction factor studies [Moon et al., 2016], and improve the understanding of the transport of firebrands, smoke, and combustion products such as carbon dioxide [see for example Kanani-Suhring and Raasch, 2017].

NUMERICAL METHODS

In LES the equations describing conservation of mass and momentum in a fluid (the continuity and Navier-Stokes equations respectively) are spatially filtered retaining the dynamically important large-scale structures of the flow. The assumption is that the largest eddies contain the most energy and therefore make the largest contribution to momentum transport. The diffusive effect of the smaller scales on the resolved large scales is non negligible and is then accounted for by using a sub-grid-scale stress model. In FDS, the filtering operation is implicit at the grid scale. That is, the numerical grid acts as a high-pass filter on the velocity. Features which have a length scale smaller than the grid size simply cannot be resolved and therefore are implicitly filtered. The use of an implicit filter can cause problems with grid independence [Sarwar et al., 2017] and overestimation of mean domain stresses [Bou-Zeid et al., 2009]. However due to the validation work previously conducted for FDS simulations of canopy flows these effects are considered negligible for these flows and the implicit filtering method is employed.

The LES equations are

$$\frac{\partial u_i}{\partial t} + u_j \left(\frac{\partial u_i}{\partial x_j} + \frac{\partial u_j}{\partial x_i} \right) = \frac{1}{\rho} \frac{\partial p}{\partial x_j} + \frac{\partial \tau_{i,j}}{\partial x_j} + F_{D,i} \,,$$

$$\frac{\partial u_i}{\partial x_j} = 0 \,,$$

where u_i is the resolved part of the velocities, $i, j = x, y, z$ are the coordinates, ρ is the fluid density, p is (the modified) pressure, and τ_{ij} is defined as:

$$\tau_{i,j} = -2(\nu + \nu_t) 2S_{i,j} + 3 \, \frac{\partial u_i}{\partial x_i} \delta_{i,j} \,,$$

where $S_{i,j}$ is the rate of strain tensor, $\delta_{i,j}$ is one if i and j are equal, and zero otherwise. The subgrid-scale stresses appear as the eddy viscosity ν_t. Here the turbulence is modelled using the constant Smagorinsky model (see, for example, Pope, 2001):

$$\nu_t = -2(C\Delta)^2 |S| S_{i,j} \,,$$

$$S_{i,j} = \frac{1}{2} \left(\frac{\partial u_i}{\partial x_j} + \frac{\partial u_j}{\partial x_i} \right) ,$$

where $\Delta = (\delta x \delta y \delta z)^{1/3}$ is a measure of grid spacing. Here we assume the constant in the Smagorinsky model is $C = 0.1$ [Lesieur et al., 2005].

A simulation domain with four canopy stripes is shown in figure 1(b). Following previous canopy simulations (eg Dupont et al. [2011], Mueller et al. [2014]) the canopy of height h is modelled as an aerodynamic drag term of the form

$$F_{D,i,k}\,(x,z) = \rho c_D \chi_k(x,z,h) \big(u_j u_j\big)^{1/2} u_i^2 .$$

We fix the value to be $c_D = 0.25$ roughly consistent with the measurements of Amiro [1990] and the study of Cassiani et al. [2008]. The function $\chi_k(x,z,h)$, defines the spatial location of the kth stripe canopy and h is constant across the stripes.

This is a simplified representation of the forest profile. In reality, there are often strong variations in LAD with height within the canopy. However, for the purposes of our idealised study we neglect that variation to isolate features caused by only the streamwise variation in LAD. For the same reasons, we choose extreme values of the LAD. A value of $LAD = 3$ is found by Amiro [1990] for a dense spruce forest, while $LAD = 0.2$ is reasonable for a eucalyptus regrowth forest [Moon et al., 2016]. In figure 1(b) green represents the uniform $LAD = 3$ canopies, and red represents the uniform $LAD = 0.2$ canopies. Four cases with these extreme differences in LAD have so far been simulated. The length scale of the stripes is then $L_c = L_x/n$ where n is the number of canopies. There are also two, four, eight, and sixteen canopy cases. The height of the canopy is taken as $h = 20$ m and h is the natural length scale of the flow.

The size of the exterior domain is chosen so that the largest relevant structures are captured. The channel sizes are chosen to follow the proportions set out by Moser et al. [1999]. The channel height is dictated by the canopy height. Bou-Zeid et al. [2009] recommends the channel height be at least four times larger than the canopy height to avoid any artificial interaction between the top boundary and the canopy. The overall domain size is $600 \times 300 \times 100$ m $(30h \times 15h \times 5h)$. The boundary conditions employed follow [Bou-Zeid et al., 2004] and are standard among most similar canopy flow simulations conducted in the literature. The streamwise and spanwise boundary conditions are periodic. The bottom (ground) boundary condition is enforced using the log-law of the wall. At the bottom of the canopy, u is small, hence canopy drag (proportional to u^2) is negligible and the log-law is appropriate here [Belcher et al., 2003]. In FDS, the log-law of the wall is enforced using a Werner-Wenkle approximation [McGrattan et al., 2013]. The top (sky) boundary condition is a free-slip condition, that is, the normal velocity vanishes at the top of the domain.

The resolution of the simulation 5 m in the horizontal directions and 0.5 stretched to 4 m at the top of the domain is chosen to be approximately three times finer than the resolution used by Bou-Zeid et al. [2009]. The flow is maintained by a constant pressure gradient of 0.005 Pa/m over the length of the channel. This gives a wind speed at the top of the domain (100 m) approximately equal to 72 km/h. This channel configuration and use of a pressure gradient driven flow to model an atmospheric surface layer is fairly standard [Bou-Zeid et al. 2004] and at the length scales considered here, the effect of the Coriolis force is negligible. The flow is initialised from a uniform velocity with a random perturbation to ensure tripping to a turbulent flow. The flow is allowed to develop to a statistically stationary state over approximately 3600 s and statistics are sampled every 2 s for 7200 s. The steady state is judged by negligible differences between instantaneous spatial mean velocities and time-averaged spatial mean velocities. The sampling time corresponds to approximately a large-eddy turnover time $t_L = h/u_h$ based on the canopy height and velocity at the canopy top. The total simulation time was selected to ensure relatively smooth derivatives of the mean velocity profiles.

RESULTS AND DISCUSSION

CHARACTERISTICS OF THE FOUR-CANOPY CASE

In this section the four-canopy case will be examined to give a representative characterisation of the flow above and within a heterogeneous tree canopy. The features of the four-canopy case are representative of all canopy cases. For all canopy cases the interesting features such as the up- and down-drafts, recirculation regions, plume structures, and variation in shear stress are periodic with a length-scale equal to two canopy lengths. For a qualitative discussion it is therefore sufficient to examine only the four-canopy case.

The results are nondimensionalised using the averaged canopy top friction velocity

$$u_* = \langle \frac{\tau}{\rho} \rangle_{t,x} = \left\langle \nu \frac{\partial u_{t,y}}{\partial z} - \langle u'w' \rangle_{t,y} \right\rangle_x ,$$

where τ is the total shear stress at the top of the canopy. Typically, in a boundary layer calculation over an unobstructed or smooth surface, the friction velocity is taken at the surface $z = 0$. In these cases the sub- and above-canopy flow are coupled and velocity scale is at the canopy top. Angled brackets denoted quantities averaged with respect to the subscripts. For example $\langle u \rangle_t$ is the time average of the u −velocity. Vertical profiles of averaged streamwise velocity are

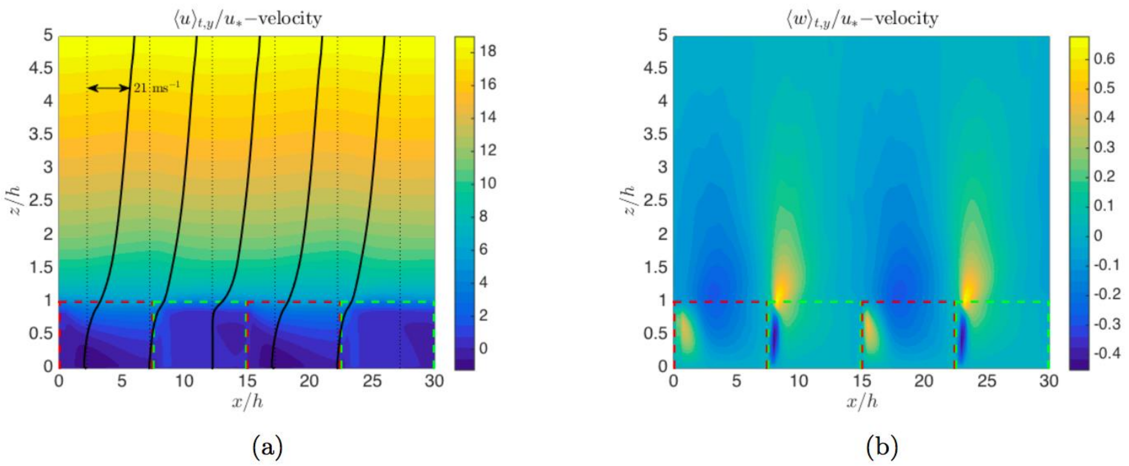

Figure 2 Contours of nondimensional average u−velocity with superimposed profiles of average u−velocity at a range of locations along the canopy. Note the contours (colours) are nondimensional but the profiles have an approximate dimensional scale as indicated. (b) Vertical velocity in the whole domain showing the strong up- (yellow) and down-drafts (blue) above and within the canopies. The canopy stripes are shown as dotted outlines.

shown at a range of locations along the four-canopy case in figure 2(a).

When the flow moves from a sparse canopy to a dense canopy the flow slows in the streamwise direction causing regions of strong upward vertical velocity above the dense canopies (figure 2(b)). Correspondingly there is a strong downward vertical velocity above the sparse canopies. The time and (xy−)mean sub-canopy flow for the homogeneous canopy cases exhibits the expected exponential decay profile predicted by Inoue [1963] and simulated by Mueller et al. [2014] and others. Within the heterogeneous canopies the sub-canopy flow exhibits a qualitatively similar decay, however, several new features exist. In particular, due to the alternating streamwise accelerations and decelerations and the consequent updrafts and down-drafts, recirculation regions are present in the sparse canopies. These recirculation regions have been previously observed at the downstream edge of a finite canopy and deep within extremely dense canopies [Cassiani et al., 2008]. The recirculation regions are visualised by plotting the streamlines of the mean flow in figure 3(a).

Similar to the flow over heterogeneous rough surfaces an internal boundary layer develops above the canopy. Immediately above the canopy 'plumes' form over each individual stripe of canopy which affects the downstream flow. The plumes are characterised by large deviations in streamwise velocity gradient from the velocity gradient averaged over all patches, that is

$$\Delta u_z = \frac{h}{u_*}\left(\frac{\partial\langle u\rangle_{t,y}}{\partial z} - \frac{\partial\langle u\rangle_{t,x,y}}{\partial z}\right).$$

Above the plume structures the overall atmospheric boundary layer flow is well mixed and the flow is homogeneous in the streamwise and spanwise directions. The critical height where this well-mixed layer commences is called the blending height. In a blended layer there will be no localised deviations from the mean flow throughout the domain. The plumes, mixed layer, and blending height above the canopy can then be visualised as shown in figure 3(b).

The contours of τ and a plot of τ in the plane above the canopy is plotted in figure 4 (a and b). The stress immediately above the canopy varies periodically over the stripes as is expected. However, in contrast to the discontinuous jumps observed over heterogeneous roughness [Bou-Zeid et al., 2004], the variation over a canopy appears to be somewhat smooth. Over the sparse canopies τ appears to approach a constant value, but over the dense canopies, τ exhibits an inflectional variation.

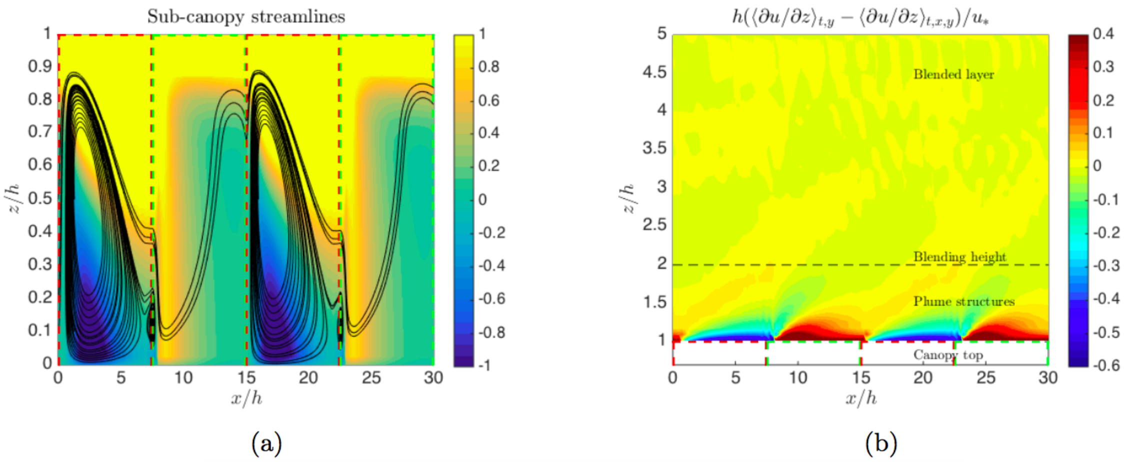

Figure 3 (a) Streamlines highlighting two recirculation vortices within the canopy. Superimposed on the nondimensional average u–velocity. (b) Contours of averaged velocity gradient difference above the canopy, clearly showing the plume structure immediately above the canopy. Above the blending height is a well-mixed boundary layer characterised by neglibible fluctuations in the velocity gradients. Sub-canopy flow is omitted from this figure. The canopy stripes are shown as dotted outlines.

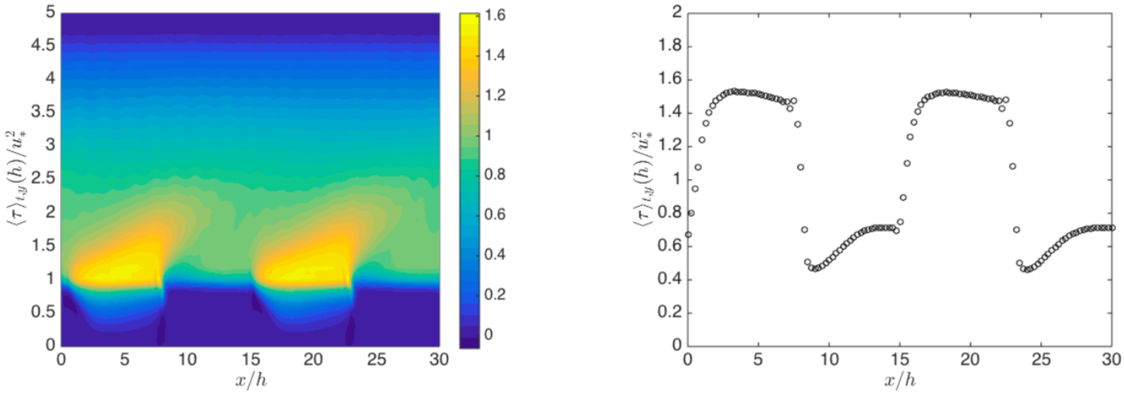

Figure 4 (a) contours of stress over the domain, (b) stress at the canopy top

BLENDING HEIGHT AND β FOR CANOPY LENGTH SCALES

The blending height is identified following Bou-Zeid et al. [2004]. In a blended layer, the difference between the domain averaged (in x, y, and t) velocity profile and the profiles of velocity averaged in y and t only is small. Plotting these profiles can then be used to identify the blending height. The upper and lower quartiles of $\langle u\rangle_{t,y} - \langle u\rangle_{t,x,y}$ are plotted, in figure 5, for each canopy case and the local minimum critical points, for $z/h > 1$, of these profiles are used to identify the blending height unambiguously. These minima points form the 'neck' of the velocity difference profile.

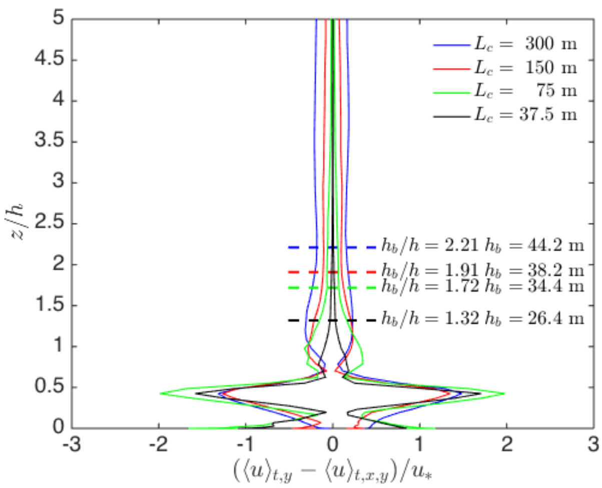

Figure 5 Upper and lower quartiles of the difference profiles. The 'neck' gives an unambiguous measurement of blending height

As the streamwise length scale of the canopies decreases (in this case, as the number of stripes increases) the blending height decreases. That is, the homogeneous boundary layer becomes closer to the canopy top. This is consistent with the idea that as the stripes become narrower, the heterogeneous canopy behaves like a uniform canopy with an average LAD value. In the case of a uniform canopy, there are no strong streamwise variations in the vertical motions above the canopy. Therefore, there is no blending height above the canopy and the flow above the canopy is homogeneous in the x- and y-directions.

A homogeneous sub-canopy flow is parameterised by $\beta = u_*/u_h$, the ratio of canopy top friction velocity to canopy top velocity [Harman and Finnigan, 2007]. In that study β was found to be approximately constant with LAD in neutral atmospheric stability conditions; the value proposed for the neutral conditions $\beta = 0.3$. In figure, 6 β as a function of x/h is plotted for all canopy cases. We also find that the mean value of β is approximately constant across the heterogeneous canopies with a value of $\beta \approx 0.2$. In the simulations of Mueller et al. [2014] $\beta \approx 0.3$ was observed for some homogeneous canopy cases. However, decreases in the measured value of β were observed for LAD profiles with extreme vertical variation (unlike the cases here where there is no vertical variation) and cases with canopy edges. Further work is required to investigate

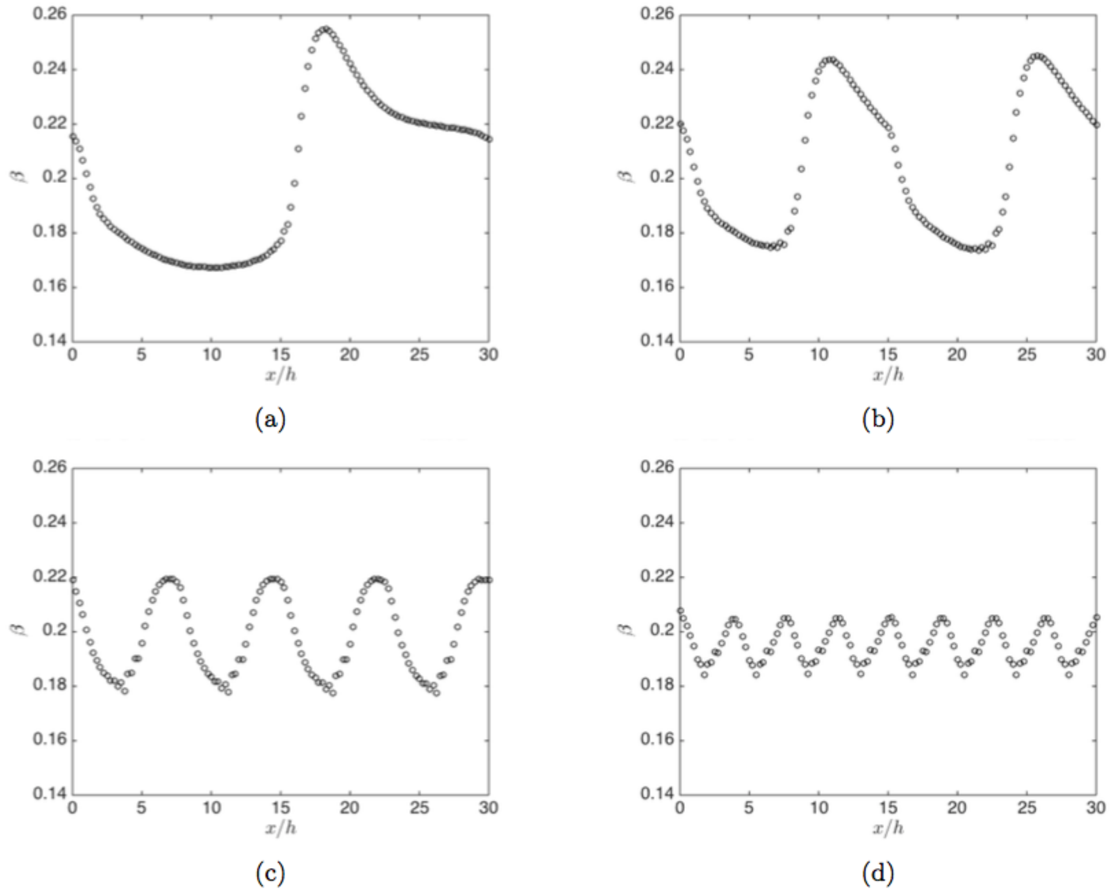

Figure 6 Variation of the β parameter for (a) two, (b) four, (c) eight, and (d) sixteen canopy cases. The mean value is approximately β = 0.2 in all cases.

the dependence of β on the canopy LAD. It is not possible to immediately extend the sub-canopy flow model of [Harman and Finnigan, 2007] because the recirculation regions which exist at the canopy interfaces will not be captured.

POTENTIAL IMPLICATIONS FOR FIRE SPREAD

Several of the features identified here may have significant effect on fire spread dynamics. Intuitively, the forward-rate-of-spread of a fire will be affected by the periodic decreases and increases of the mean sub-canopy wind speed. That is, within the sparse canopies, the McArthur model would predict a higher rate-of-spread (RoS) than in the dense canopies. However, this implies that the fire will accelerate between the alternating canopy stripes. The McArthur model, like almost all empirical fire models, assumes that the fire is spreading at a quasi-steady rate. How the accelerating fire is driven by the spatially varying sub-canopy wind speed is unclear. As the canopies become narrower, the fire has less distance over which to accelerate or slow down. The RoS may in fact remain roughly constant even though the sub-canopy wind speed is varying considerably over a short distance.

We also expect that smoke, firebrand transport, and spotfire ignition to be influenced by the strong updrafts and recirculation regions which occur at canopy boundaries. Previous work by Kanani-Suhring and Raasch, [2017] showed canopy boundaries lead to enhanced concentrations (of for example CO_2) in the lee side of a canopy. Analogously, boundaries between dense and sparse forests may also lead to enhanced concentrations of smoke and combustion products in these regions. Furthermore, the strong updrafts on the leading dense canopy edges and the large downdrafts over sparse canopies are likely to enhance firebrand lofting, at dense canopy leading edges, and falling firebrand distribution over sparse canopies. Therefore, spotfire ignition may occur more frequently in the sparse canopy regions, near an inhomogeneity in the canopy, because a greater number of firebrands land there relative to the rest of the canopy.

Small spot fire ignitions may be significantly influenced by recirculation regions. Simpson et al. [2013] found that recirculation in the lee side of hills can lead to lateral spread of large fires spreading over the hill. The magnitude of velocities in lee vortices is larger than observed in canopy recirculation regions, and therefore we expect that only small fires may be influenced by the canopy recirculation vortices. Therefore this effect may be significant in spotfire ignition and growth. It is unlikely that the recirculation regions will persist in the presence of a large buoyant fire plume which will disturb the background wind flow in the vicinity of the fire.

All of these effects must be rigorously studied in further simulation work before any useful conclusions may be drawn.

CONCLUSIONS

Large eddy simulations of flow over heterogeneous canopies have been conducted. The streamwise velocity profiles follow the inflectional profile typical of flows over canopies [Harman and Finnigan, 2007]. However, at the canopy interfaces prominent recirculation regions are observed, similar to the recirculation region which exists downstream of a finite canopy [Cassiani et al., 2008]. The vertical velocity exhibits up- and down-drafts corresponding to the dense and sparse canopies respectively.

For heterogeneous canopies the mean β appears to be slightly lower than measured experimentally for homogeneous canopies, and does not appear to vary significantly with the number of canopies. For the heterogeneous cases the time and domain mean flow exhibits a flow reversal, or a recirculation close to the ground. At the boundary at the dense-to-sparse canopy interfaces, a velocity couplet and a corresponding recirculating structure are formed inside the sparse canopy.

The data set presented here will be used to develop a parameterisation of the boundary layer above a heterogeneous tree canopy and it will also be used to model the sub-canopy flow. The determination of an equivalent blending height, displacement length, and surface roughness length in terms of the canopy parameters can be used in surface schemes of numerical weather prediction models which will improve the overall wind forecast accuracy. The development of a reduced model of sub-canopy winds in heterogeneous forests will be useful to wildfire management agencies that require estimates of sub-canopy wind speeds for operational fire models such as the McArthur model or the Rothermel [Rothermel, 1972] model. A particular question that arises from this study is the effect of recirculation regions on fire spread. Recirculation regions may not persist in the presence of a fire plume. It is possible to simulate the effects of the canopy on a fire spreading under a canopy using FDS and this is the subject of a forthcoming study. Simulations will be conducted to understand the effect the canopy has on the forward-rate-of-spread of a fire and examine if the recirculation regions influence the fire spread. Extending this work will contribute to understanding the effect of forest heterogeneities on firebrand and smoke transport.

ACKNOWLEDGEMENTS

The authors are grateful to the administrators of Spartan, a high-performance computing cluster at the University of Melbourne.

REFERENCES

B.D. Amiro. Comparison of turbulence statistics within three boreal forest canopies. Boundary-Layer Meteorology, 51(1-2):99–121, 1990.

SE Belcher, N Jerram, and JCR Hunt. Adjustment of a turbulent boundary layer to a canopy of roughness elements. Journal of Fluid Mechanics, 488:369–398, 2003.

E. Bou-Zeid, C. Meneveau, and M.B. Parlange. Large-eddy simulation of neutral atmospheric boundary layer flow over heterogeneous surfaces: Blending height and effective surface roughness. Water Resources Research, 40(2), 2004.

E. Bou-Zeid, J. Overney, B. D. Rogers, and M. B. Parlange. The effects of building representation and clustering in large-eddy simulations of flows in urban canopies. Boundary-layer meteorology, 132(3):415–436, 2009.

M. Cassiani, G.G. Katul, and J.D. Albertson. The effects of canopy leaf area index on airflow across forest edges: large-eddy simulation and analytical results. Boundary-layer meteorology, 126(3):433–460, 2008.

S. Dupont, J-M. Bonnefond, M. R. Irvine, E. Lamaud, and Y. Brunet. Long-distance edge effects in a pine forest with a deep and sparse trunk space: in situ and numerical experiments. Agricultural and Forest Meteorology, 151(3):328–344, 2011.

E.R. Grant, A.N Ross, B.A. Gardiner, and S.D. Mobbs. Field observations of canopy flows over complex terrain. Boundary-Layer Meteorology, 156(2):231–251, 2015.

I.N. Harman and J. J. Finnigan. A simple unified theory for flow in the canopy and roughness sublayer. Boundary-layer meteorology, 123(2):339–363, 2007.

S. Heemstra, Rural Fire Service of NSW, personal communication, 2015.

E. Inoue. On the turbulent structure of airflow within crop canopies. Journal of the Meteorological Society of Japan. Ser. II, 41(6):317–326, 1963.

F. Kanani-Suhring and S. Raasch. Enhanced scalar concentrations and fluxes in the lee of forest patches: A large-eddy simulation study. Boundary-Layer Meteorology, pages 1–17, 2017.

M. Lesieur, O.Metais, and P. Comte. Large-eddy simulations of turbulence. Cambridge University Press, 2005.

A.G. McArthur. Fire behaviour in eucalypt forests. Department of National Development Forestry and timber Bureau. Leaflet 107, 1967

K. McGrattan, S. Hostikka, and J.E. Floyd. Fire dynamics simulator, users guide. NIST special publication, 1019, 2013.

K. Moon, T.J. Duff, and K.G. Tolhurst. Sub-canopy forest winds: understanding wind profiles for fire behaviour simulation. Fire Safety Journal, 2016.

R.D. Moser, J. Kim, and N.N. Mansour. Direct numerical simulation of turbulent channel flow up to Re= 590. Phys. Fluids, 11(4):943–945, 1999.

E. Mueller, W. Mell, and A. Simeoni. Large eddy simulation of forest canopy flow for wildland fire modeling. Canadian Journal of Forest Research, 44(12):1534–1544, 2014.

R.C. Rothermel. A mathematical model for predicting fire spread in wildland fuels. USDA Forest Service Research Paper INT-115, 1972.

M. Sarwar, M.J. Cleary, K.A.M. Moinuddin, and G.R. Thorpe. On linking the filter width to the boundary layer thickness in explicitly filtered large eddy simulations of wall bounded flows. International Journal of Heat and Fluid Flow, 65:73–89, 2017.

F. Schlegel, J. Stiller, A. Bienert, H-G.Maas, R. Queck, and C. Bernhofer. Large-eddy simulation study of the effects on flow of a heterogeneous forest at sub-tree resolution. Boundary-Layer Meteorology, 154(1):27–56, 2015.

C.C. Simpson, J.J., Sharples, J.J., J.P, Evans, and M.F., McCabe, 2013. Large eddy simulation of atypical wildland fire spread on leeward slopes. *International Journal of Wildland Fire*, *22*(5), pp.599-614.

K. Tolhurst, B. Shields, and D. Chong, 2008. Phoenix: development and application of a bushfire risk management tool, The *Australian Journal of Emergency Management*, *23*(4), p.47.